Journal of Information & Communication Technology
Vol. 5, No. 1, (Spring 2011) 30-29

A Robust Local Model for Segmentation Based on Coefficient of Variation

Ghulam Murtaza*
Haider Ali*
Noor Badshah*
Department of Basic Sciences, UET Peshawar

ABSTRACT

Many image segmentation models work efficiently when segmenting images with prominent edges and regions but often we need to segment images with low contrast, unilluminated objects, inhomogeneity problems and images with overlapping region of almost homogeneous intensities.
In fact these mentioned images pose challenges to the existing models. In this paper, we proposed a new variational model for image segmentation, based on a robust local statistical information.
In contrast with the existing models, the experimental results validate that the new proposed model is robust in terms of accurate detection in such tough images.

INSPEC Classification : A4230V, B6135, C1250M, C5260B

Keywords : Segmentation, Level Set, Functional Minimization, Coefficient of Variation (CoV), Total Variation.

1. INTRODUCTION

Image segmentation is a fundamental task and central problem among image processing application and computer vision. The aims of image segmentation is to extract objects from background and convert it into classes or categories, corresponding to different regions. After segmenting the images, each pixel should belong to only one class. In other words, image segmentation is used to partition the given image into different objects, each having some similar features, e.g, color, intensity and texture. There are several approaches to solve image segmentation problems, such as watershed algorithms (J. Weickert and G. Kuhne, 2003), region growing and emerging (R. Adams and L. Bischof, 1994), minimum description length criteria (Y. Leclerc, 1990), and Mumford-Shah (MS) energy minimization (D. Mumford and J. Shah, 1989). Recently, PDE-based active contour models (T. F. Chan and L. A. Vese, 2001)(M. Kass, A. Witkin and D. Terzopoulos, 1988)(L. A. Vese and T. F. Chan, 2002) for curve evolution have been popular for image segmentation. In a few decade years, a variety of image segmentation models based on variational techniques have been introduced. Mathematically these image segmentation models are well studied and are defined in continuous setting.

The MS model was firstly proposed as a general image segmentation model by Mumford and Shah in (D. Mumford and J. Shah, 1989). The goal of the MS energy functional is to segment a given image u into different regions in terms of intensity, color, texture etc. The MS general energy functional is given by:

* The material presented by the authors does not necessarily portray the viewpoint of the editors and the management of the Institute of Business and Technology (IBT) or Shaheed Zulfiqar Ali Bhutto Institute of Science & Technology, Karachi, Pakistan.

*Ghulam Murtaza : murtaza uop99@yahoo.com
*Haider Ali : haider uop99@yahoo.com
*Noor Badshah : noor2knoor@gmail.com

$$F(u, K)^{MS} = \int_{\Omega} (u - u_0)^2 dxdy + \alpha \int_{\Omega - K} |\nabla u|^2 dxdy + \beta \int_K ds. \tag{1}$$

where Ω is a bounded domain in $\mathbb{R}^n, u : \Omega$ [0, 1] is a given image. The first term in (1) is called fidelity term which penalize the difference between the smooth image u_0 and the original image *u*, keeping remaining constraints (terms) in consideration. The second term is called regularizer which helps to give *u* smooth in the region $\Omega - K$ inside the prominent edges. The third is the length term, which helps to shorten edges as possible so that edges look straight. Where α and β are positive (tuning) parameters. With this mechanism, whenever an image u_0 is segmented, an image *u* is obtained with smooth regions and clear sharp edges. In other words, a cartoon version of a given image is obtained.

The second well known variational image segmentation model is the active contour model or snakes model, proposed by Kass et al in (M. Kass, A. Witkin and D. Terzopoulos, 1988), has proved an efficient structure for image segmentation. The main idea of active contour model is to start initially with a curve around the object to be detected, and the curve moves toward the boundary of the object. The snake model of (M. Kass, A. Witkin and D. Terzopoulos, 1988) aims to find the segmentation curve *C* (in parametric form with $C(s) : [0, 1] \rightarrow \mathbb{R}^2$) by solving the problem

$$\min_C F_3(C) = \int_0^1 \alpha |C'(s)|^2 + \beta |C''(s)| - \lambda |\nabla u_0(C(s))|^2 ds. \tag{2}$$

One of the chief draw backs of this technique is, its sensitivity to initial contour and the difficulties arisen from topological changes like the merging and splitting of the evolving curve. Since the Snakes model was proposed, many methods have been proposed to modify it, in which level set method proposed by Osher and Sethian (S. Osher and J. A. Sethian,1988) is the most popular and successful one.

An energy functional in variational models for image segmentation usually consist two main energy functionals, known as external energy and internal energy. An external energy functional helps to drive the active contour towards the actual boundaries of an object, whereas internal energy functional helps to maintain the smoothness of the active curve. In region based variational models of image segmentation, the external energy is usually the data fidelity term. In most of the variational region based models(X. F. Wang, D. S. Huang, H. Xu, 2012)(N. Badshah and K. Chen, 2010)(T. F. Chan and L. A. Vese, 2001) a fidelity term embeds the image data in energy functional using the concept of statistic variance.

2. THE CHAN-VESE MODEL (CV

We organized this paper in the following way. Section 2 describe a review of the Chen-Vese model (T. F. Chan and L. A. Vese, 2001). Section 3 reveals a latest segmentation model (X. F. Wang, D. S. Huang, H. Xu, 2012). In Section 4 we present our proposed model for image segmentation and derive the Euler-Lagrange equation. Section 5 exhibits experimental results.

T. F. Chan and L. A. Vese (T. F. Chan and L. A. Vese, 2001)proposed an active contour region based model.

The proposed energy functional of the CV model is given by:

$$F(\Gamma, c_1, c_2) = \int_{inside(\Gamma)} |z - c_1|^2 dx + \int_{outside(\Gamma)} |z - c_2|^2 dx + \mu(length(\Gamma)), \tag{3}$$

where Γ is a variable curve with a given $z(x, y)$ and c_1, c_2 are constant approximations of $z(x, y)$ inside and outside Γ respectively.

In level set formulation (S. Osher and J. A. Sethian,1988)(J. A. Sethian, 1999), the equation (3) is given as :

$$F(\phi, c_1, c_2) = \mu \int_\Omega \delta(\phi)|\nabla\phi|dxdy + \lambda_1 \int_\Omega |z(x,y) - c_1|^2 H(\phi)dxdy + \lambda_2 \int_\Omega |z(x,y) - c_2|^2(1 - H(\phi))dxdy, \quad (4)$$

where ϕ is a level set function, H(·) is the Heaviside function and $\delta(\cdot)$ is the Dirac delta function.

Minimization of $F(\phi, c_1, c_2)$ with respect to c_1 and c_2, yields

$$c_1(\phi) = \frac{\int_\Omega z(x,y)H(\phi)dxdy}{\int_\Omega H(\phi)dxdy}, \qquad c_2(\phi) = \frac{\int_\Omega z(x,y)(1 - H(\phi))dxdy}{\int_\Omega (1 - H(\phi))dxdy},$$

assuming that the curve has nonempty interior and exterior in Ω .

By using regularized versions of H and δ , denoted by H_ϵ and δ_ϵ , with $\delta_\epsilon . = H'_\epsilon$,

$$H_\epsilon(x) = \frac{1}{2}(1 + \frac{2}{\pi}\arctan(\frac{x}{\epsilon}), \qquad \delta_\epsilon(x) = H'_\epsilon(x) = \frac{\epsilon}{\pi(\epsilon^2 + x^2)},$$

the regularized version of $F(\phi, c_1, c_2)$ is denoted as $F_\epsilon(\phi, c_1, c_2)$.

Minimization of F_ϵ respect to ϕ yields the Euler-Lagrange equation for ϕ :

$$\begin{cases} \delta_\epsilon(\phi)\Big[\mu \text{div}\Big(\frac{\nabla\phi}{|\nabla\phi|}\Big) \\ -\lambda_1(z(x,y) - c_1)^2 + \lambda_2(z(x,y) - c_2)^2\Big] = 0 & \text{in } \Omega, \\ \frac{\delta_\epsilon(\phi)}{|\nabla\phi|}\frac{\partial\phi}{\partial\vec{n}} = 0 & \text{on } \partial\Omega, \end{cases} \quad (5)$$

where $\vec{n}$ is an exterior unit normal to the boundary $\partial\Omega$ and $\frac{\partial\phi}{\partial\vec{n}}$ is the normal derivative of ϕ at boundary (T. F. Chan and L. A. Vese, 2001). Then once ϕ is found, the piecewise segmented image is given by

$$u(x,y) = H(\phi(x,y))c_1 + (1 - H(\phi(x,y)))c_2.$$

The CV model work well in images free of en-homogeneity problems and in such case c_1 and c_2 are good approximations of *z* inside and outside the dynamic curve Γ respectively. However, in images acquired with low frequencies, unilluminated objects, overlapping regions of homogeneous intensities, the performance of the CV model is very devastating. The experimental results in section 5 validate this discussion.

3. THE LOCAL CHAN-VESE MODEL (LCV)

To modify the CV model for images with intensity inhomogeneity, X-F. Wang et el (X. F. Wang, D. S. Huang, H. Xu, 2012) proposed LCV model by incorporating their local statistical functional in the CV energy functional.

The proposed regularized energy functional of the LCV model in level set formulation is given by:

$$\begin{aligned} F_\epsilon(\phi, c_1, c_2, d_1, d_2) &= \mu \int_\Omega \delta_\epsilon(\phi)|\nabla\phi|dxdy + \int_\Omega \frac{1}{2}(|\nabla\phi| - 1)^2 dxdy \\ &+ \lambda_1 \int_\Omega (z - c_1)^2 H_\epsilon(\phi)dxdy + \lambda_1 \int_\Omega (z - c_2)^2(1 - H_\epsilon(\phi))dxdy \\ &+ \lambda_2 \int_\Omega (z^* - d_1)^2 H_\epsilon(\phi)dxdy + \lambda_2 \int_\Omega (z^* - d_2)^2(1 - H_\epsilon(\phi))dxdy. \end{aligned} \quad (6)$$

where $\mu,\ \lambda_1,\ \lambda_2$ are constants and are used for assigning different weights and $z^*(x,y)$ denotes the difference image $g_k * z(x,y) - z(x,y)$ where g_k is an averaging convolution operator of window size $k \times k$.

The first term $\int_\Omega \delta_\epsilon(\phi)|\nabla\phi|dxdy$ of the energy functional given in (6) is a regularizer term that helps to maintain the smoothness of the active curve.

The second term $\int_\Omega (z-c_1)^2 H_\epsilon(\phi)dxdy + \int_\Omega (z-c_2)^2(1-H_\epsilon(\phi))dxdy$ is a global term which helps the active contour to capture the main structure of objects/regions an image. The third term $\int_\Omega (z^* - d_1)^2 H_\epsilon(\phi)dxdy + \int_\Omega (z^* - d_2)^2(1 - H_\epsilon(\phi))dxdy$ is a local term which contributes in detecting small and valuable details.

In similar lines to section 2, minimization of $F_\epsilon(\phi, c_1, c_2, d_1, d_2)$ leads to the following solutions,

$$
\begin{aligned}
c_1(\phi) &= \frac{\int_\Omega z(x,y)H_\epsilon(\phi)dxdy}{\int_\Omega H_\epsilon(\phi)dxdy}, \qquad c_2(\phi) = \frac{\int_\Omega z(x,y)(1-H_\epsilon(\phi))dxdy}{\int_\Omega (1-H_\epsilon(\phi))dxdy}, \\
d_1(\phi) &= \frac{\int_\Omega z^*(x,y)H_\epsilon(\phi)dxdy}{\int_\Omega H_\epsilon(\phi)dxdy}, \qquad d_2(\phi) = \frac{\int_\Omega z^*(x,y)(1-H_\epsilon(\phi))dxdy}{\int_\Omega (1-H_\epsilon(\phi))dxdy},
\end{aligned}
$$

and

$$
\begin{aligned}
\frac{\partial\phi}{\partial t} &= \delta_\epsilon(\phi)\Big[-\lambda_1(z-c_1)^2 - \lambda_2(z^*-d_1)^2 + \lambda_1(z-c_2)^2 + \lambda_2(z^*-d_2)^2\Big] \quad (7) \\
&+ \Big[\mu\delta_\epsilon(\phi)\nabla.\Big(\frac{\nabla\phi}{|\nabla\phi|}\Big) + \Big(\nabla^2\phi - \nabla.\frac{\nabla\phi}{|\nabla\phi|}\Big)\Big], \quad in\ \Omega \\
\phi(x,y,t) &= \phi_0(x,y,0), \quad in\ \Omega.
\end{aligned}
$$

The LCV model work well in many images effected with image inhomogeneity problems. However, our experimental results revealed that low contrast images, images acquired with low frequencies, unilluminated objects, overlapping regions of homogeneous intensities the performance of the LCV model is not satisfactory. The experimental results in section 5 validate this discussion very well.

4. THE PROPOSED COEFFICIENT OF VARIATION BASED SEGMENTATION MODEL (PSM)

In the PSM, we will use the coefficient of variation *CoV* as a fidelity term instead of variance which can be mostly seen as a fidelity term in existing region based models (X. F. Wang, D. S. Huang, H. Xu, 2012)(N. Badshah and K. Chen, 2010)(T. F. Chan and L. A. Vese, 2001). In contrast with the existing models, experimental results using *CoV* as a fidelity term in the PSM show best result in terms of accurate detection.

Based on the concept of coefficient of variation *CoV* (S. E. Ahmed, 1995)(M. Mora, C. Tauber, H. Batatia, 2005), we propose a new model for image segmentation given by:

$$
\begin{aligned}
F(\Gamma, c_1, c_2, d_1, d_2) &= \mu(length(\Gamma)) \quad (8) \\
&+ \lambda_1 \int_{inside(\Gamma)} \frac{(z-c_1)^2}{c_1^2}dx + \lambda_1 \int_{outside(\Gamma)} \frac{(z-c_2)^2}{c_2^2}dx \\
&+ \lambda_2 \int_{inside(\Gamma)} \frac{(z^*-d_1)^2}{d_1^2}dx + \lambda_2 \int_{outside(\Gamma)} \frac{(z^*-d_2)^2}{d_2^2}dx,
\end{aligned}
$$

where $\mu, \lambda_1, \lambda_2$ are constants and are used for assigning different weights and $z^*(x,y) = g_k * z(x,y) - z(x,y)$.

The PSM for a given discrete image z may be explained as follows:
By denoting the image intensity value at position (i,j) as $z_{i,j}$, the variance is defined as:

$$Var(z) = \frac{1}{N}\sum_{i,j}\Big(z_{i,j} - Mean(z)\Big)^2,$$

which can be seen as a fidelity term used in many existing models (X. F. Wang, D. S. Huang, H. Xu, 2012)(N. Badshah and K. Chen, 2010)(T. F. Chan and L. A. Vese, 2001), whereMean(z) denotes the mean intensity of a given image.

The *CoV* is defined as:

$$CoV^2 = \frac{Var(z)}{\Big(Mean(z)\Big)^2}$$

The value of *CoV* is smaller in uniform areas than the areas where there are edges [15, 19]. It means that a smaller value indicates that pixels belong to the uniform region and larger value indicates that pixels belong to the edges. The properties of *CoV* (M. Mora, C. Tauber, H. Batatia, 2005) (M. A. Schulze and Q. X. Wu.,1995) imply that it can be used as a good region descriptor, that is, it can be used as a image data fidelity term. The experimental results ensure that the performance of the PSM is far better than the existing CV and the LCV models in segmenting the challenging images.

Thus we consider the regularized problem in level set formulation as

$$\min_{\phi,c_1,c_2,d_1,d_2} F_\epsilon(\phi,c_1,c_2,d_1,d_2),$$

where

$$\begin{aligned} F_\epsilon(\phi,c_1,c_2,d_1,d_2) &= \mu\int_\Omega \delta_\epsilon(\phi)|\nabla\phi|dxdy \\ &+ \lambda_1\int_\Omega \frac{(z-c_1)^2}{c_1^2}H_\epsilon(\phi)dxdy + \lambda_1\int_\Omega \frac{(z-c_2)^2}{c_2^2}(1-H_\epsilon(\phi)) \\ &+ \lambda_2\int_\Omega \frac{(z^*-d_1)^2}{d_1^2}H_\epsilon(\phi)dxdy + \lambda_2\int_\Omega \frac{(z^*-d_2)^2}{d_2^2}(1-H_\epsilon(\phi))dxdy. \end{aligned}$$

In similar lines to section 2, minimization of $F_\epsilon(\phi,c_1,c_2,d_1,d_2)$ leads to the following solutions,

$$c_1(\phi) = \frac{\int_\Omega z^2(x,y)H_\epsilon(\phi)dxdy}{\int_\Omega z(x,y)H_\epsilon(\phi)dxdy}, \qquad c_2(\phi) = \frac{\int_\Omega z^2(x,y)(1-H_\epsilon(\phi))dxdy}{\int_\Omega z(x,y)(1-H_\epsilon(\phi))dxdy},$$

$$d_1(\phi) = \frac{\int_\Omega (z^*)^2(x,y)H_\epsilon(\phi)dxdy}{\int_\Omega z^*H_\epsilon(\phi)dxdy}, \qquad d_2(\phi) = \frac{\int_\Omega (z^*)^2(x,y)(1-H_\epsilon(\phi))dxdy}{\int_\Omega z^*(1-H_\epsilon(\phi))dxdy},$$

and

$$\begin{aligned} \frac{\partial\phi}{\partial t} &= \delta_\epsilon(\phi)\Big[\mu\nabla.\Big(\frac{\nabla\phi}{|\nabla\phi|}\Big) \qquad (9)\\ &+ \lambda_1\Big(-\frac{(z-c_1)^2}{c_1^2} + \frac{(z-c_2)^2}{c_2^2}\Big) + \lambda_2\Big(-\frac{(z^*-d_1)^2}{d_1^2} + \frac{(z^*-d_2)^2}{d_2^2}\Big)\Big], \quad in\ \Omega \\ \phi(x,y,t) &= \phi_0(x,y,0), \quad in\ \Omega. \end{aligned}$$

By using the AOS method as done in (T. Lu, P. Neittaanmaki, and X. C. Tai, 1991)(J. Weickert, B. M. ter Haar Romeny and M. A. Viergever, 1998)(J. Weickert and G. Kuhne, 2003) to solve the PDE (9), the following system of equations is obtained:

$$\begin{aligned}(I - 2\Delta t A_l(\Phi^k))\Phi_l^{k+1} &= f^k, for\ l = 1, 2,\\ and\ \Phi_l^{k+1} &= \frac{1}{2}\sum_{l=1}^{2}\Phi_l^{k+1},\end{aligned}$$

where I is the identity matrix and A_l f or $l = 1$, 2 a tridiagonal matrix.

5. EXPERIMENTAL RESULTS

In this section we present some experimental results. The experiments show that the new method PSM performs better when segmenting low contrast images, images with fuzzy edges, images with homogeneous overlapping regions.

In the start, we demonstrate comparison of the proposed PSM model with the CV model, and secondly we give some experimental results to compare the proposed PSM with the LCV model. For clarity, we shall denote by

M-1 . the CV model
M-2 . the LCV model and
M-3 . the proposed PSM model.

The figure 1 displays a real brain image and the performance of M-1 and M-3. The figures 1(b), 1(c), 1(e) and 1(f) exhibit clearly the performance of M-1 and the proposed M-3 model. It can be easily observed that the M-3 is robust in accuracy. In addition, the segmented result 1(e) and 1(f) ensure the quality of detection of the proposed method.

The figure 2 shows a synthetic image with the performance of M-1 and M-3. In each of the figures 2(b), 2(c), 2(e) and 2(f), the performance of M-1 and M-3 can easily interpreted that M-3 is robust in accurate detection.

The figure 3 displays a synthetic image and the performance of M-2 and M-3. In contrast with M-2, the figures 3(b), 3(c), 3(e) and 3(f) clearly exhibit that the proposed M-3 is robust in accurate detection. The same conclusions can be derived from figures ?? by observing the figures 4(b), 4(c), 4(e), 4(f), 5(b), 5(c), 5(e) and 5(f)that M-2 fails to complete the task and the performance of M-3 is robust in accuracy.

Fig. 1
Segmenting a real brain image, using the M-1 method and the proposed M-3 method: (a) Initial contour; (b) Result of M-1 model; (c) Segmented Result; (d) Initial contour; (e) Result of M-3 model; (f) Segmented Result; size=256 X 256.

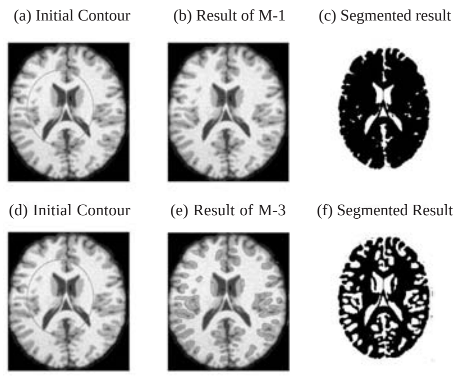

Fig. 2
Segmenting a synthetic image, using M-1 method and M-3 method: (a) Initial contour; (b) Result of M-1 model; (c) Segmented Result; (d) Initial contour; (e) Result of M-3 model; (f) Segmented Result; size=256 X 256.

(a) Initial Contour (b) Result of M-1 (c) Segmented result

(d) Initial Contour (e) Result of M-3 (f) Segmented Result

Fig. 3
Segmenting a synthetic image, using M-2 method and the proposed M-3 method: (a) Initial contour; (b) Result of M-2 model; (c) Segmented Result; (d) Initial contour; (e) Result of M-3 model; (f) Segmented Result; size=256 X 256.

(a) Initial Contour (b) Result of M-2 (c) Segmented result

(d) Initial Contour (e) Result of M-3 (f) Segmented Result

Fig. 4
Segmenting a synthetic image, using M-2 and M-3: (a) Initial contour; (b) Result of M-2 model; (c) Segmented Result; (d) Initial contour; (e) Result of M-3 model; (f) Segmented Result; size=256 X 256.

(a) Initial Contour (b) Result of M-2 (c) Segmented result

(d) Initial Contour (e) Result of M-3 (f) Segmented Result

Fig. 5
Segmenting a hardware image, using the M-2 method and the M-3 method: (a) Initial contour; (b) Result of M-2 model; (c) Segmented Result; (d) Initial contour; (e) Result of M-3 model; (f) Segmented Result; size=256 X 256.

(a) Initial Contour (b) Result of M-2 (c) Segmented result

(d) Initial Contour (e) Result of M-3 (f) Segmented Result

6. CONCLUSION

A new model of image segmentation is proposed which utilizes both local and global image information using local statistical functional and coefficient of variation. The experimental results validate that this new model is robust in accurate detection than the existing segmentation models.

REFERENCES

R. Adams and L. Bischof (1994). Seeded region growing. IEEE Trans. Pattern Analysis and Machine Intelligence, 16(6):641-647.

S. E. Ahmed (1995). A pooling methodology for coefficient of variation. Sankhya: The Indian Journal of Statistics, 57(B1):57.75.

N. Badshah and K. Chen (2010). Image Selective Segmentation under Geometrical Constraints Using an Active Contour Approach. Math. Comp., 7:759.778.

V. Caselles, R. Kimmel and G. Sapiro (1997). Geodesic active contours. International Jornal of Computer Vision, 22(1):61.79.

T. F. Chan and L. A. Vese (2001). Active contours without edges. IEEE Transactions on Imag Processing, 10(2):266.277.

K. Chen (2005). Matrix Preconditioning Techniques and Applications. Cambridge University Press.

L. D. Cohen (1991). On active contour models and balloons. In Computer Vision, Graphics, and Image Processing: Image Understanding, 53(2):211.218.

C. L. Guyader and C. Gout. (2008). Geodesic active contour under geometrical conditions theory and 3D applications. Numerical Algorithms, 48:105-133.

C. Gout, C. L. Guyader and L. A. Vese (2005). Segmentation under geometrical conditions with geodesic active contour and interpolation using level set method. Numerical Algorithms, 39:155-173, 2005.

M. Jeon, M. Alexander, W. Pedrycz, and N. Pizzi (2005) Unsupervised hierarchical image segmentation with level set and additive operator splitting. PRL., 26(10):1461-1469.

M. Kass, A. Witkin and D. Terzopoulos (1988). Snakes: active Contours Models. International Jornal of Computer Vision, 1:321.331.

Y. Leclerc (1990). Region growing using the MDL principle, In: DAPPRA Image Understanding Workshop.

Y. B. Li and J. S. Kim (2011). Multiphase image segmentation using a phase-field model. Computers and Mathematics with Applications, 62:737.745.

T. Lu, P. Neittaanmaki, and X. C. Tai (1991). A parallel splitting up method and its application to Navier-Stokes equations Appl. Math. Lett., 4(2):25-29.

M. Mora, C. Tauber, H. Batatia (2005). Robust level set for heart cavities detection in ultrasound images Computers in Cardiology, 32:235-238.

D. Mumford and J. Shah (1989). Optimal approximation by piecewise smooth functions and associated variational problems. Communications on Pure Applied Mathematics, 42:577.685.

S. Osher and R. Fedkiw (2005). ¥Ã-Level Set Methods and Dynamic Implicit Surfaces, Springer Verlag, 2003 Lec. Notes Comp. Sci., 3708:499-506.

S. Osher and J. A. Sethian (1988). Fronts propagating with curvature-dependent speed: algorithms based on Hamilton-Jacobi formulations. J. Comput. Phys., 79(1):12.49.

M. A. Schulze and Q. X. Wu. (1995). Nonlinear edge-preserving smoothing of synthetic aperture radar images. Proceedings of the New Zealand Image and Vision Computing 95 Workshop, pp.65. 70.

J. A. Sethian (1999). Level set methods and fast marching methods. Evolving interfaces in Computational Geometry, Fluid Mechanics, Computer Vision and Material Science, Cambridge University Press.

L. A. Vese and T. F. Chan (2002). A multiphase level set framework for image segmentation using the Mumford and Shah model, Int. J. Computer Vision, 50(3):271-293.

L. Vincent and Soille (1994). Watersheds in Digital Spaces - an efficient algorithm based on immersion. IEEE Trans. Pattern Analysis and Machine Learning, 6:583-598.

X. F. Wang, D. S. Huang, H. Xu (2012). An efficient local Chan-Vese model for image segmentation. Pattern Recognition , 43:603.618, 2010.

J. Weickert and G. Kuhne (2003). Fast methods for implicit active contours models. In: Geometric Level SetMethods in Imaging, Vision, and Graphics, pp.43-58, 2003.

J. Weickert, B. M. ter Haar Romeny and M. A. Viergever (1998). Efficient and reliable schemes for nonlinear diffusion filtering, IEEE Trans. Image Proc., 7:398-410.

Y. Yu and S. T. Acton (2004). Edge detection in ultrasound imagery using the instantaneous coefficient of variation. IEEE Transactions On Image Processing 13(12):1640.1655.